Biosensors and Bioelectronics 228 (2023) 115220

Contents lists available at ScienceDirect

Biosensors and Bioelectronics

journal homepage: www.elsevier.com/locate/bios

Low-cost, facile droplet modification of screen-printed arrays for internally validated electrochemical detection of serum procalcitonin

Paulo Roberto de Oliveira [a,b], Robert D. Crapnell [a], Alejandro Garcia-Miranda Ferrari [a], Phatsawit Wuamprakhon [a,c], Nicholas J. Hurst [a], Nina C. Dempsey-Hibbert [a], Montree Sawangphruk [c], Bruno Campos Janegitz [b], Craig E. Banks [a,*]

[a] Faculty of Science and Engineering, Manchester Metropolitan University, Chester Street, M1 5GD, United Kingdom
[b] Laboratory of Sensors, Nanomedicine and Nanostructured Materials, Federal University of São Carlos, Araras, 13600-970, Brazil
[c] Centre of Excellence for Energy Storage Technology (CEST), Department of Chemical and Biomolecular Engineering, School of Energy Science and Engineering, Vidyasirimedhi Institute of Science and Technology, Rayong, 21210, Thailand

ARTICLE INFO

Keywords:
Electrochemistry
Screen-printed electrodes (SPE)
Biosensor
Procalcitonin (PCT)
Sepsis
Screen-printed arrays

ABSTRACT

This manuscript presents the design and facile production of screen-printed arrays (SPAs) for the internally validated determination of raised levels of serum procalcitonin (PCT). The screen-printing methodology produced SPAs with six individual working electrodes that exhibit an inter-array reproducibility of 3.64% and 5.51% for the electrochemically active surface area and heterogenous electrochemical rate constant respectively. The SPAs were modified with antibodies specific for the detection of PCT through a facile methodology, where each stage simply uses droplets incubated on the surface, allowing for their mass-production. This platform was used for the detection of PCT, achieving a linear dynamic range between 1 and 10 ng mL^{-1} with a sensor sensitivity of 1.35×10^{-10} NIC%/ng mL^{-1}. The SPA produced an intra- and inter-day %RSD of 4.00 and 5.05%, with a material cost of £1.14. Internally validated human serum results (3 sample measurements, 3 control) for raised levels of PCT (>2 ng mL^{-1}) were obtained, with no interference effects seen from CRP and IL-6. This SPA platform has the potential to offer clinicians vital information to rapidly begin treatment for "query sepsis" patients while awaiting results from more lengthy remote laboratory testing methods. Analytical ranges tested make this an ideal approach for rapid testing in specific patient populations (such as neonates or critically ill patients) in which PCT ranges are inherently wider. Due to the facile modification methods, we predict this could be used for various analytes on a single array, or the array increased further to maintain the internal validation of the system.

1. Introduction

Sepsis has been recognised as a global health priority by the United Nations World Health Assembly, due to estimates of more than 19 million cases and 6 million sepsis-related deaths occurring worldwide annually (Fleischmann et al., 2016). It is characterised by widespread organ damage due to the patient's hyperinflammatory immune system response to the infection. Thus, sepsis is defined as life-threatening organ dysfunction due to a dysregulated host response (Singer et al., 2016). Full diagnosis of sepsis requires both evidence of bloodstream infection (BSI) and systemic inflammation and currently, the testing methods involve lengthy laboratory procedures, including blood culture testing, which can take up to 72 h. However, in patients with sepsis, for every hour that treatment is not initiated, there is a 7.6% reduction in the patient's chances of survival (Kumar et al., 2006), highlighting the need for rapid, simple and accurate near-patient testing.

Procalcitonin (PCT) is a U.S. Food and Drug Administration (FDA) approved biomarker for the assessment of the progression of infection to sepsis, for aiding in decisions for antibiotic therapy for some patients, and also for the potential de-escalation of antibiotics for septic patients if tracked over time (de Jong et al., 2016; Faix et al., 2013; Pierrakos and Vincent, 2010). PCT is a 116-amino acid polypeptide that is commonly championed in the identification of bacterial infections due to its wide biological range, short time of induction after bacterial stimulus, and long half-life (Dandona et al., 1994; Moyer, 2012). Indeed, a wealth of literature demonstrates the utility of PCT in the identification and

* Corresponding author.
E-mail address: c.banks@mmu.ac.uk (C.E. Banks).

https://doi.org/10.1016/j.bios.2023.115220
Received 23 January 2023; Received in revised form 27 February 2023; Accepted 7 March 2023
Available online 11 March 2023
0956-5663/© 2023 The Authors. Published by Elsevier B.V. This is an open access article under the CC BY license (http://creativecommons.org/licenses/by/4.0/).

monitoring of sepsis and has led to a number of large systematic reviews justifying its inclusion in standard care pathways for sepsis (Liu et al., 2015; Malik et al., 2021; Patnaik et al., 2020). Recently, Jones et al., (2021) have shown that PCT provided the earliest indicator of bacterial sepsis in a study investigating the serial measurement of PCT as well as specific platelet indices, lactate (Crapnell et al., 2021b) and another FDA-approved biomarker C-Reactive Protein (CRP) in critically ill adult patients (Wacker et al., 2013). PCT levels have also been shown to be significantly elevated in neonates (Chiesa et al., 1998) and paediatrics (Lautz et al., 2016) with infections, and it can therefore be used for early diagnosis in these cohorts. It should be noted that baseline levels of PCT are higher in neonates than that seen in adults (Sachse et al., 1998). Concentrations of PCT have been stratified to aid interpretation; current NHS guidelines consider the normal range in adult populations to be $<$ 0.05 ng mL^{-1}, with $<$0.50 ng mL^{-1} considered to represent a low risk of sepsis, and concentrations $>$2.0 ng mL^{-1} considered to represent a high risk of sepsis. However, it is well established that there are many 'special' patient groups such as trauma patients, burns patients and those with renal dysfunction in which serum PCT may be elevated at baseline and then may increase further in the presence of infection, and as such, higher thresholds for diagnosis need to be considered (Meisner et al., 1998; Smith et al., 2020). This is especially true of the neonatal population. Indeed, there is a post-natal physiological increase in the serum PCT level in all neonates with a peak value at 24 h after birth. Therefore, for serum PCT testing to be applicable for neonates in the clinical setting, it has been necessary to derive distinct reference ranges (Fukuzumi et al., 2016). Naramura et al. (Naramura et al., 2020), have recently shown that median PCT levels within the 95% range 12–36 h after birth are 1.05 ng mL^{-1}. The same study also showed that during the height of systemic bacterial infection, median concentrations of PCT can reach ≈50 ng mL^{-1}, with some patients expressing levels over ten-fold higher than this median. Currently, PCT can be measured in serum samples on specialised clinical chemistry analysers within hospital pathology laboratories. PCT clinical cut-offs and algorithms were originally established using the global reference method BRAHMS PCT sensitive KRYPTOR assay (Thermo Scientific) (Soni et al., 2013). For this reason, several manufacturers have implemented BRAHMS PCT assays on their own instruments using raw materials from BRAHMS GmbH, and all BRAHMS PCT assays are calibrated to the BRAHMS PCT sensitive KRYPTOR assay. Six license partner assays are currently available including Abbott (Architect and Alinity analyzers), Biomerieux (Vidas analyzer), Diasorin (Liaison analyzer), Fujirebio (Lumipulse analyzer), Roche (Cobas analyzer), and Siemens (Centaur and Atellica analyzers). All of these are sandwich immunoassays, but the method of detection varies between analysers. All of the above have reporting times of approximately 20 min, but this is based on the time from sample loading onto the analyser to the time of the result being produced. It does not account for the significant time incurred in transporting samples from the ICU or other clinical wards for remote testing in a busy hospital pathology laboratory, where samples running through such large analysers are also being tested for several other analytes which increases reporting times. Furthermore, the logistical issues with remote testing of blood samples, means that serial monitoring of PCT over time during the acute phase of hyperinflammation is difficult and therefore not routinely practiced by clinicans, despite its obvious clinical advantages.

There are a plethora of analytical techniques reported in the literature for the detection of PCT, such as photoluminescence (Kokorina et al., 2021), electrochemiluminescence (Fang et al., 2021), fluorescence (Qi et al., 2016), surface plasmon resonance (Sener et al., 2013), dynamic light scattering (Zhu et al., 2022), surface-enhanced Raman scattering (Chen et al., 2020), and electrochemical sensors (La, 2020; Nellaiappan et al., 2021). The utilisation of electrochemistry for the quantification of analytes is extremely popular due to its simple measurement procedure, and short response times, whilst still providing excellent sensitivity and selectivity (Bard et al., 2022; Compton and Banks, 2018). It can be seen throughout the literature for a wide range of applications such as heavy metal detection (Ariño et al., 2022; Crapnell and Banks, 2022; Ferrari et al. 2020, 2022), food a drink safety (Crapnell and Banks, 2021b; Ferrari et al., 2021a; Honeychurch and Piano, 2018; Mannino and Wang, 1992), and healthcare (Crapnell et al., 2022a; Crapnell and Banks, 2021a; Hernández-Rodríguez et al., 2020; Vinoth et al., 2021). Unsurprisingly, electrochemical biosensors represent a significant proportion of biosensor research due to the advantages offered through electrochemistry combined with the inherent selectivity offered by biological recognition elements (Crapnell and Banks, 2021c). The success of electrochemical biosensors can be seen as a delicate balance between achieving the low limits of detection (LODs) whilst keeping production costs down. These two factors account for the different trends observed in the literature of electrochemical biosensors: 1) a movement toward the incorporation of micro- or nanomaterials, in many cases multiple materials, into the biosensor to improve LODs (Crapnell and Banks, 2021c), and 2) a movement away from classical electrodes such as glassy carbon, Au and Pt solid electrodes toward cheaper alternatives such as screen-printed electrodes (SPEs) which negates the need to polish the classical electrodes prior to use (Ferrari et al., 2021b). SPEs are fabricated by depositing inks on the substrate material in a layer-by-layer fashion, offering an economical yet highly reproducible, disposable and robust system that often comprises the entire three-electrode basic configuration in one small, flat platform (typically a few cm^2) (Crapnell et al., 2022a). These electrodes can be produced using various ink materials, as with solid electrodes, such as Au, Pt and carbon, whereby for biosensors the choice is often governed by the desired bio-recognition element modification procedure or once again, the cost.

SPEs, comprised typically of a graphite working electrode are among the most material cost-effective to produce and are therefore attractive for the mass-production of electrochemical biosensors. The attachment of recognition elements for biosensing can be achieved in different ways such as adsorption, covalent bonding, electrochemical deposition and electrochemical polymerisation (Pérez-Fernández et al., 2020). Covalent attachment of antibodies to SPE surfaces has been achieved in the literature through, firstly, deposition of a suitable linking group, such as electro-grafting of a diazonium salt, followed by EDC/NHS coupling of the antibody (Crapnell et al., 2021a, 2021c). However, the formation of a dense monolayer of aryl groups on the surface is notoriously difficult utilising this method, often leading to significant blocking of electrode surfaces, a reduction in the obtained current and, therefore, a decrease in sensitivity of the platform. Rodríguez-González et al., (2020) recently reported the self-limiting covalent modification of carbon surfaces through a droplet immobilisation method. This methodology limits the forest-like growth of diazonium salts on the surface of the electrode (Partington et al., 2018), which should lead to beneficial electrochemical performance.

Herein, we show the production of a screen-printed array (SPA), containing six carbon working electrodes, for the detection of PCT in undiluted human serum samples. All modifications steps are performed utilising only droplets of solution, highlighting how reliable electrochemical biosensors can be produced in a facile, automated way. The synergy between the low-cost, mass-manufacturing nature of SPEs and the simple droplet modification highlights the attractiveness of the system for commercial production. Additionally, the in-built control of the SPA could offer a route toward the rapid indication of sepsis in an ICU environment, allowing for treatment to be initiated more quickly and increasing the chance of patient survival.

2. Experimental section

2.1. Chemicals

All chemicals used of analytical grade and were used as received without any further purification. All solutions were prepared with deionised water of resistivity not less than 18.2 MΩ cm from a Milli-Q

Integral 3 system from Millipore UK (Watford, UK). Hexaaminer-uthenium (III) chloride (RuHex, 98%), potassium hexacyanoferrate (II) trihydrate (98.5–102.0%), potassium hexacyanoferrate (III) (99%), potassium chloride (99.0–100.5%), L-ascorbic acid (99%), 4-aminobenzoic acid (4-AB, >99%), sodium nitrite (>97%), bovine serum albumin (BSA, >98%), N-(3-dimethylaminopropyl)-N′-ethylcarbodiimide hydrochloride (EDC, >99%), N-hydroxysuccinimide (NHS, 98%), human serum from human male AB plasma, hydrochloric acid and phosphate-buffered saline (PBS) tablets were purchased from Merck (Gillingham, UK). Procalcitonin Human recombinant protein and specific antibody were purchased from Abcam PLC (Cambridge, UK).

2.2. Screen-printed electrode production

Graphite screen-printed electrode arrays (SPAs) were produced in-house using a stencil design through a layer-by-layer process. Firstly, a graphite ink (Product Ink: C2000802P2; Gwent Electronic Materials Ltd, Pontypool, UK) was deposited onto a flexible polyester film (250 μm thickness, Autostat, Milan, Italy) using a DEK 248 screen printer machine (DEK, Weymouth, UK) before being cured in a fan oven at 60 °C for 30 min. Secondly, an Ag|AgCl reference was printed in place using screen-printing Ag|AgCl paste (Product Code: D2070423D5; Gwent Electronic Materials Ltd, Pontypool, UK), which was again cured in a fan oven at 60 °C for 30 min. Finally, a dielectric ink layer (Product Code: D2070423D5; Gwent Electronic Materials Ltd., Pontypool, United Kingdom) was printed onto the system and again cured in a fan oven at 60 °C for 30 min. Following these steps, the SPAs were ready for use with six working electrodes of 3.1 mm diameter, a counter electrode with an exposed area of 37 mm^2 and a printed Ag|AgCl *pseudo*-reference of area 17.25 mm^2.

2.3. Biosensor production

The working electrodes (WEs) of the SPA were prepared with a facile modification methodology using sequential droplets. Firstly, a diazonium modification was applied to the graphitic working electrodes through sequential droplets (González et al., 2020). A 5 μL droplet of 4-AB (4 mM) and sodium nitrite (100 mM) in HCl (50 mM) was applied to the surface of the WEs for 10 min, followed by the application of 5 μL droplet of L-ascorbic acid (4 mM) at pH 3.8 for a further 10 min. The WEs were thoroughly cleaned by rinsing with PBS (pH = 5.0). The diazonium layer was then activated using EDC/NHS coupling through the application of a 10 μL droplet of EDC (100 mM) and NHS (20 mM) in PBS (pH = 5.0) for 1 h. The WEs were then thoroughly cleaned by rinsing with PBS (pH = 7.4). The procalcitonin specific antibody was then attached to the surface of the WEs through the application of a 10 μL droplet of PCT-Ab (10 μg mL^{-1}) for 3 h at 4 °C. The WEs were then thoroughly cleaned by rinsing with PBS (pH = 7.4). Finally, the excess available surface of the WEs were blocked through the application of a 10 μL droplet of BSA (0.5 wt%) for 30 min. Once washed once more with PBS (pH = 7.4), the SPAs were stored in PBS in the fridge until use.

2.4. Physiochemical characterisation

X-ray Photoelectron Spectroscopy (XPS) data were acquired using an AXIS Supra (Kratos, UK), equipped with a monochromated Al X-ray source (1486.6 eV) operating at 225 W and a hemispherical sector analyser. It was operated in fixed transmission mode with a pass energy of 160 eV for survey scans and 20 eV for region scans with the collimator operating in slot mode for an analysis area of approximately 700 × 300 μm, the FWHM of the Ag $3d_{5/2}$ peak using a pass energy of 20 eV was 0.613 eV. Before analysis, each sample was ultrasonicated for 15 min in propan-2-ol and then dried for 2.5 h at 65 °C as this has been shown in our unpublished data to remove excess contamination and therefore minimise the risk of misleading data. The binding energy scale was calibrated by setting the adventitious sp^3 C 1s peak to 285.0 eV; this calibration is acknowledged to be flawed (Greczynski and Hultman, 2021), but was nonetheless used in the absence of reasonable alternatives, and because only limited information was to be inferred from absolute peak positions.

Scanning Electron Microscopy (SEM) measurements were recorded on a Supra 40VP Field Emission (Carl Zeiss Ltd., Cambridge, UK) with an average chamber and gun vacuum of 1.3×10^{-5} and 1×10^{-9} mbar respectively. Samples were mounted on the aluminum SEM pin stubs (12 mm diameter, Agar Scientific, Essex, UK). To enhance the contrast of these images, a thin layer of Au/Pd (8 V, 30 s) was sputtered onto the electrodes with the SCP7640 from Polaron (Hertfordshire, UK) before being placed in the chamber.

2.5. Electrochemical experiments

A Multi Autolab M204 potentiostat (Utrecht, the Netherlands) was used in conjunction with NOVA 2.1.5 (Utrecht, the Netherlands) to carry out all electrochemical measurements on the screen-printed array (SPA). The SPAs were comprised of the carbon working electrodes (Ø = 3.1 mm), carbon counter electrode and Ag|AgCl paste reference electrode. These were connected to the potentiostat via an edge connector (RS Components, Corby, UK). Solutions were degassed thoroughly with nitrogen prior to any electrochemical measurement.

Scan rate studies against RuHex (1 mM in 0.1 M KCl) were performed using cyclic voltammetry (CV, 5-150 mV s^{-1}) between +0.20 V to -0.35 V vs. Ag|AgCl printed pseudo-reference, while for $[Fe(CN)_6]^{3-/4-}$ (1 mM in 0.1 M KCl), CV was performed (20 mV s^{-1}) between +0.5 V to -0.3 V.

Electrochemical Impedance Spectroscopy (EIS) was performed in $[Fe(CN)_6]^{3-/4-}$ (1 mM in 0.1 M KCl) at the formal potential, E_f, measured previously by CV (~+0.14 V). This was performed in the frequency range between 100,000–0.1 Hz, with an amplitude of 0.01 A and 10 frequencies per decade.

Spiked serum samples were produced by mixing 5 μL of appropriate procalcitonin stock solution to 495 μL of commercially purchased human serum sample. This was mixed using a vortex mixer and used to incubate onto the SPA's for 15 min.

2.6. Additive manufacturing

The design and .3 MF file for the solution holder on the SPA was drawn in Autodesk® Fusion 360®, then sliced and converted to a. GCODE file using PrusaSlicer (Prusa Research, Prague, Czech Republic). The solution holder was then produced using a Prusa i3 MK3S+ 3D-printer (Prusa Research, Prague, Czech Republic) using Fused Filament Fabrication (FFF) technology. It was printed using Prusament Galaxy Silver poly(lactic acid) (PLA, Prusa Research, Prague, Czech Republic), with a nozzle size of 0.4 mm, first layer temperature of 215 °C, print temperature of 210 °C, bed temperature of 60 °C, 100% infill and 0.15 mm layer height. To seal the sample holder, Nitrile Rubber O-ring Cord (RS Components, Corby, UK) was attached to the inner edge and clamped firmly using M3 screws (RS Components, Corby, UK).

3. Results and discussion

The production of low-cost, reproducible and reliable sensing platforms for the identification of vital biomarkers is of urgent need for near-patient-testing (Crapnell et al., 2022b). Screen-printing of carbon-based electrodes offers an affordable and mass-producible base for electrochemical sensing, however many reported biosensors can struggle with reliability or sensitivity. The utilisation of various micro- or nanomaterials to overcome poor electrode kinetics created by the blocking of the electrode surface through the dense formation of linking layers has been reported, and while effective, this significantly increases the production cost of the platform (Crapnell and Banks, 2021c; Partington et al., 2018). In this work we aim to address both issues above by

offering an alternative, facile methodology for the deposition of a thin linking layer, and through the use of a screen-printed array (SPA) provide internally validated results with each sensor.

3.1. Design, production and characterisation of the screen-printed array (SPA)

The process for the production of the SPA is outlined in Fig. 1A, where it can be seen that a system is produced with six individual graphite working electrodes, alongside a common graphite counter electrode and Ag|AgCl ink reference electrode. Firstly, the graphite ink layer is deposited onto the flexible polyester substrate (Foster et al., 2014), establishing the working and counter electrodes, and the connections for every electrode, including the reference. It can be seen that for each set of three, the outer working electrodes have a slightly slanted connection. This allowed for adequate isolation between the working electrodes for individual modifications and the correct separation between the connection tabs for the insertion into a standard commercial edge connector. As reported, the shorter connection length would be expected to have enhanced electrochemical performance (Whittingham et al., 2021), however the difference of 0.1 mm is shown later to be negligble. Onto the graphite layer, a small layer of Ag|AgCl ink is applied where the reference will be exposed to the solution. Finally, onto this, a dielectric layer is deposited to insulate the connections and define the electrode areas. A photograph of the finished SPA can be seen in Fig. S1.

To confirm the morphology of the graphite working electrodes SEM was performed, Fig. 1B. It can be seen that the surface of the working electrodes consists of a mixture of small particles and large flakes, corresponding to the binder materials and graphite respectively, which is consistent with other graphite screen-printed working electrodes seen throughout the literature (Galdino et al., 2015; Hallam et al., 2010). To confirm the chemical composition of the graphitic working electrodes XPS was performed. The C 1s spectrum, Fig. 1C, exhibits a large asymmetric peak at 284.5 eV, which is consistent with the XPS emission found for graphitic carbon species alongside a smaller high-binding energy peak at 290.8 eV arising from the π-π* transitions within the graphitic carbon (Blume et al., 2015; Gengenbach et al., 2021). The other carbon environments present on the surface of the working electrode are attributed to the organic binder used within the commercial graphite ink.

To ensure the reproducibility of the SPA production, electrochemical testing was initially performed using the near-ideal outer sphere redox probe hexaammineruthenium (III) chloride which allows for the accurate determination of the electroactive area (A_e) and heterogeneous electrochemical rate constant (k^0), Fig. S2A (Crapnell and Banks, 2021d; García-Miranda Ferrari et al., 2018). Fig. 2A presents an example of the obtained scan rate study (5–150 mV s^{-1}) for a single working electrode, where a one-electron reduction process is observed followed by a one-electron oxidation on the reverse scan. Fig. 2B, highlights the average cathodic peak current obtained over the testing of 5 different SPAs, with the standard deviation calculated by using the individual cathodic peak current for the six individual working electrodes per SPA. It can be seen that there is both excellent intra- and inter-array reproducibility. Utilising the data obtained for all electrodes on multiple SPA's, the A_e and k^0 were calculated to be (0.065 ± 0.002) cm^2 and (0.0109 ± 0.0003) cm s^{-1} respectively. The low relative standard deviations (RSD) values obtained for both these parameters (3.64% and 5.51%) respectively, indicate the reproducibility of the manufacturing process of the SPA's. The intra-array reproducibility is further emphasised through cyclic voltammetric (CV, ν = 20 mV s^{-1}) and electrochemical impedance spectroscopy (EIS) measurements performed against the common inner-sphere redox probe $[Fe(CN)_6]^{3-/4-}$, Fig. S2B, Fig. 2C and D respectively. For the CV, the measured cathodic peak current and peak-to-peak separation (ΔE_p) were calculated to have a %RSD of 4.22% and 3.48%, respectively. Fitting of the Nyquist plots obtained by EIS with the appropriate Randles circuit as seen in Fig. 2D, the average R_s and R_{CT} values obtained for an intra-array were (1790 ±

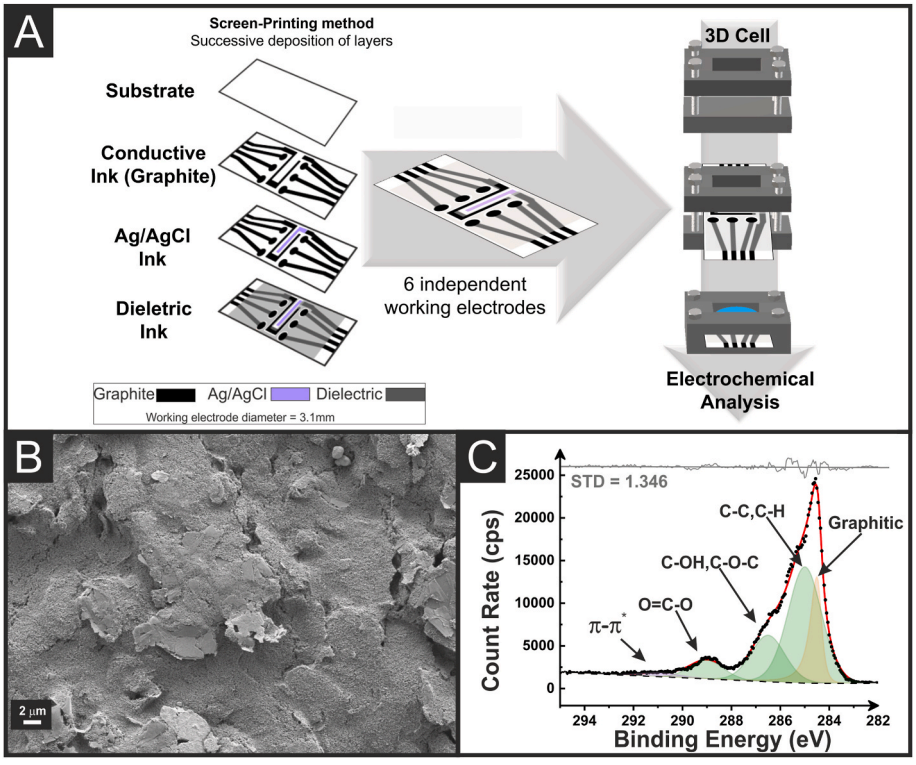

Fig. 1. A) Schematic representation of the screen-printed array production and connection to 3D-printed sample holder. **B)** SEM image of the screen-printed array working electrode at 5000x magnification. **C)** XPS C 1s spectrum for the screen-printed array working electrode.

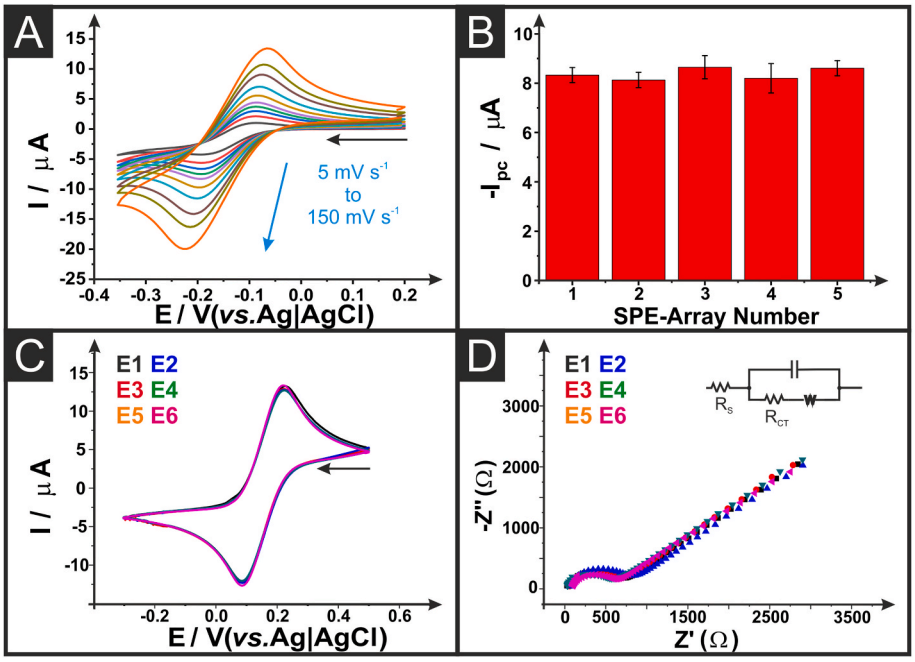

Fig. 2. A) Cyclic voltammograms (5–150 mV s^{-1}) of hexaaminеruthenium (III) chloride (1 mM, 0.1 M KCl) using the SPA comprising of graphite working and counter electrode and Ag|AgCl paste reference electrode. **B)** Plot showing the peak cathodic current (20 mV s^{-1}) obtained across 5 SPA's, with the error calculated from the 6 electrodes comprising the single SPA. **C)** Cyclic voltammograms (20 mV s^{-1}) from the 6 working electrodes on a single SPA for $[Fe(CN)_6]^{3-/4-}$ (1 mM, 0.1 M KCl). **D)** Nyquist plots (100,000–0.1 Hz, $E_{app} = E_f$) from the 6 working electrodes on a single SPA for $[Fe(CN)_6]^{3-/4-}$ (1 mM, 0.1 M KCl).

160) Ω and (820 ± 70) Ω, respectively. This confirms the connection length of the SPA to be shorter than a standard in-house SPE (Whittingham et al., 2021). Electrochemical characterisation using standard outer- and inner-sphere redox probes have highlighted the excellent performance and reproducibility of the electrodes, with no significant difference observed between the central and outer electrodes in the array. We now progress to the development of the biosensing array for the determination of procalcitonin (PCT).

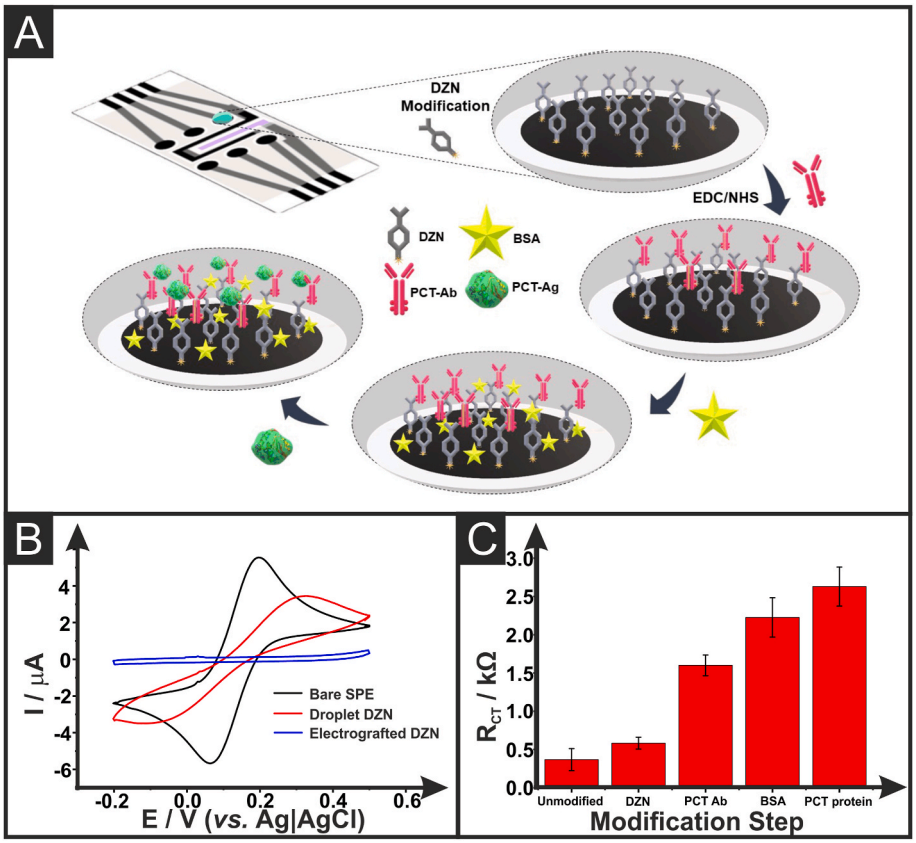

Fig. 3. A) Schematic of the biosensor droplet modification process. **B)** Cyclic voltammograms (20 mV s^{-1}) comparing the response to $[Fe(CN)_6]^{3-/4-}$ (1 mM, 0.1 M KCl) for an unmodified, droplet modified and electrodeposition-modified graphite working electrode. **C)** Comparison of the charge-transfer resistance of $[Fe(CN)_6]^{3-/4-}$ (1 mM, 0.1 M KCl) for each modification step in the biosensor production using the droplet methodology.

3.2. Droplet modification of SPA for biosensing

Electrodeposition of a diazonium salt (either amine or carboxyl terminated) onto a working electrode surface, followed by conventional coupling chemistry, is a common way to achieve covalent attachment of antibodies (Crapnell et al., 2022a; Crapnell et al., 2021a). This methodology requires each working electrode to go through the electrodeposition modification, where typically a dense linking layer is created, which significantly negatively effects the electrochemical performance of the electrode (Partington et al., 2018). As such, we propose the use of a facile droplet electrode modification system, Fig. 3A, where the initial linking group is covalently attached to the graphite working electrode through the application of two solutions together (González et al., 2020).

Firstly, the attachment of the diazonium linking layer to the graphite working electrodes was explored by comparing the droplet methodology and electrodeposition on the SPA's. Briefly, the droplet methodology involved the placement of a 5 μL droplet of diazonium salt solution onto the graphite working electrode, followed by a second 5 μL droplet of ascorbic acid solution and incubation for 10 min, Fig. S3. This process is performed to form a dense, well-defined monolayer of carboxyl-terminated aryl groups covalently bound to the surface (González et al., 2020). Fig. 3B exhibits the CV obtained in $[Fe(CN)_6]^{3-/4-}$ (1 mM, 0.1 M KCl) for working electrodes unmodified, and modified through droplets and electrodeposition. It can be seen that in both cases, there is a reduction in the current values. For the droplet modified electrode, the redox process of $[Fe(CN)_6]^{3-/4-}$ is still visible but with a reduction in the anodic peak current from 5.58 μA to 4.34 μA, and a significant increase in the ΔE_p from 163 mV to 219 mV. This suggests that there is a surface modification of the electrode, hindering the electron transfer from $[Fe(CN)_6]^{3-/4-}$, but it is still possible. In contrast, no redox process can be observed when using the working electrode modified through electrodeposition. This indicated that a far denser layer aryl layer was deposited on the surface, not allowing the inner-sphere probe to access the electrode surface.

Following the successful modification of the SPA working electrode surface with the carboxyl-terminated aryl group, the rest of the modification for the biosensor was performed and tracked through EIS. Fig. 3C highlights the increase in the R_{CT} measured on the corresponding Nyquist plots. It can be seen that the R_{CT} increases significantly for each step of the modification, antibody immobilisation, and BSA blocking, indicating further blocking of the electrode surface. This increase in R_{CT} can also be seen in the addition of the PCT protein, indicating that recognition and binding to the target are occurring. Overall, the material cost of producing the SPA biosensing platform was £1.14.

3.3. Electroanalytical performance of droplet-modified SPA

Detection of PCT using the SPA was first performed in PBS (pH = 7.4) to establish the electroanalytical performance of the sensor. A different concentration of PCT (1–100 ng mL^{-1}) was incubated on each electrode on three separate SPA's, followed by EIS analysis in $[Fe(CN)_6]^{3-/4-}$ (1 mM). The Nyquist plots corresponding to one SPA are presented in Fig. 4A, where is can be seen that there is a a large increase in the profile as the concentration of PCT is raised. To produce a suitable calibration plot the normalised impedance change (NIC%), calculated using results obtained across 3 separate SPA's, is plotted against the concentration of PCT, shown in Fig. 4B. A linear dynamic range (LDR) can be seen between 1 and 10 ng mL^{-1}, with a second linear section of a significantly reduced gradient between 10 and 100 ng mL^{-1}. The sensor achieved a sensitivity of 1.35×10^{-10} NIC%/ng mL^{-1} and Limit of Detection (LOD) of 0.7 ng mL^{-1}. Additionally, the intra- and inter-day (7 days) reproducibility of the system was tested, producing %RSD of 4.00% and 5.05%, respectively. This sensor is compared to others reported in the literature in Table S1. The wide analytical range of the current sensor makes it suitable for the analysis of PCT in special patient groups such as neonates, in which PCT values are inherently higher than normal at baseline. However, we propose that both the LOD and LDR of the system could be improved through the incorporation of additional macro- or nanomaterials (Crapnell and Banks, 2021c), or through the increased loading of antibodies onto the surface (Crapnell et al., 2022a), which would make a sensor that would be suitable for assessing low and high risk sepsis in more general adult population.

To verify the ability of the proposed system to diagnose a possible sepsis case via PCT, spiked human serum samples were analysed. To achieve this both low (2 ng mL^{-1}) and high (50 ng mL^{-1}) PCT spiked serum samples were analysed, Fig. 5 A and B respectively. For these tests three working electrodes were used as controls and three were used for sample analysis. This gave the ability to internally validate whether there was a real increase in the measured NIC%. It can be seen that in both cases, there is a significant increase in the NIC% from the controls with much larger increases for the higher concentrations of PCT, as expected. It can be seen that from SPA to SPA there are significant variations in the absolute value of the NIC%, which is expected to come from a combination of the nature of the complicated matrix and natural variations in antibody orientation. To ensure the selectivity of the sensor, identical experiments were performed with the incubation of common interferents C-reactive protein (CRP) and interleukin-6 (IL-6), Fig. 5C. It can be seen that there was no change in the NIC% across multiple SPA's, and this highlights the selectivity of the system when compared to the results for 2 ng mL^{-1} PCT.

Here we report the design, production, facile modification and use of a 6-working electrodes SPA for the detection of serum PCT levels. The SPA is created in a simple, mass-producible way, modified by simply using droplets of solution making biosensor production highly automatable. This has the potential to be a low-cost, mass-producible way to create reliable, internally validated biosensing platforms. The SPA removes issues requiring absolute accuracy on the concentration of analyte and allows for future production of a traffic light sensor system, where the presence of increased serum levels of PCT can be identified

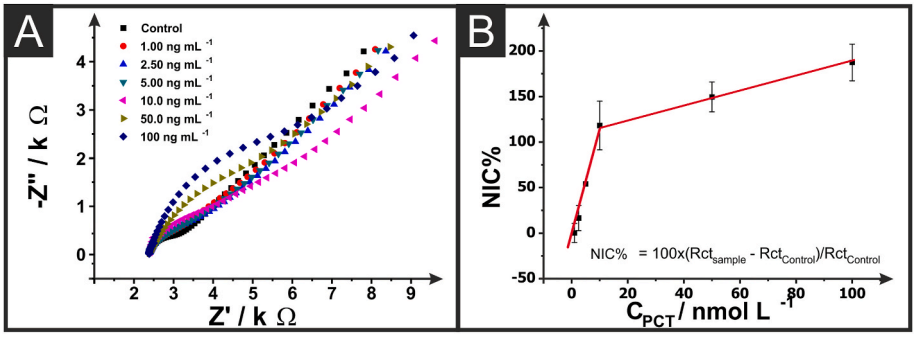

Fig. 4. A) Nyquist plots in $[Fe(CN)_6]^{3-/4-}$ (1 mM, 0.1 M KCl) for the addition of PCT (1–100 ng mL^{-1}) to the modified SPA. **B)** Analytical curve corresponding to the addition of PCT (1–100 ng mL^{-1}) to the modified SPA.

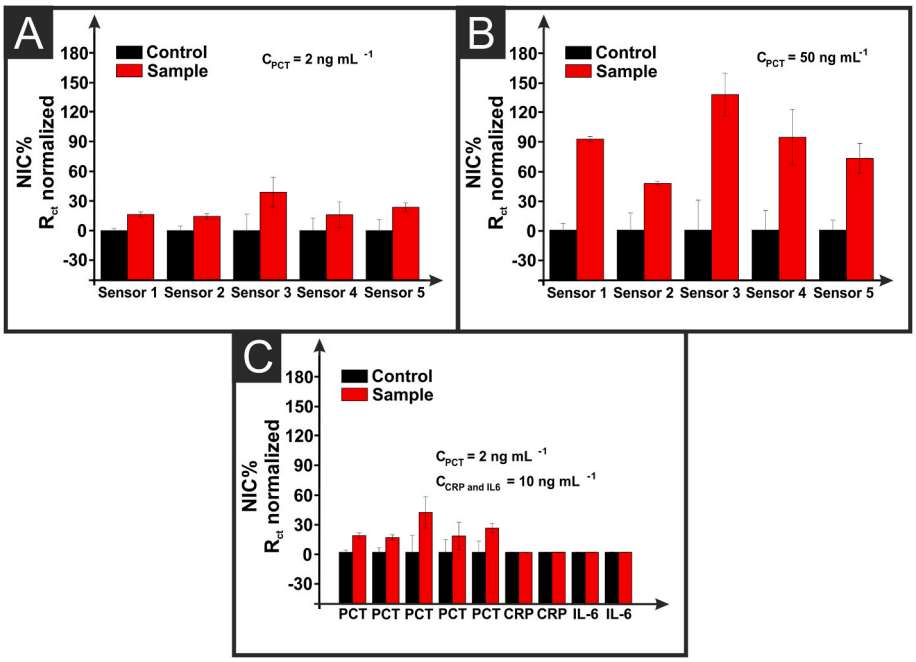

Fig. 5. A) Plot of response of 5 different SPA to PCT (2 ng mL^{-1}) alongside their respective internal controls. **B)** Plot of response of 5 different SPA to PCT (50 ng mL^{-1}) alongside their respective internal controls. **C)** Plot of response of 5 different SPA to PCT (2 ng mL^{-1}) alongside their respective internal controls, along with the response of 2 separate SPAs to both CRP and IL-6 (10 ng mL^{-1}) alongside their internal controls.

readily from comparison with the control. This could offer clinicians vital information to rapidly begin treatment for "query sepsis" patients while awaiting results from more lengthy remote laboratory testing methods. Additionally, due to the facile modification methods we predict this could be used for various analytes on a single array, or the array increased further to maintain the internal validation of the system.

A limitation of the work with regards to suitability for near-patient testing is the focus on testing of serum samples; It is acknowledged that the most convenient near-patient tests allow for analysis of whole blood to minimise sample preparation requirements, yet many current CE-marked near-patient tests involve analysis of serum or plasma. Furthermore, before such technology can be realized, it is important to work towards accurate and sensitive detection of target analytes in a simpler medium (serum), before moving on to adapting the approach for testing in more complex whole blood samples, particularly since PCT reference ranges used as a basis for this work have themselves been derived in serum samples.

4. Conclusions

This manuscript presents the design and facile production of screen-printed arrays (SPAs) for the internally validated determination of raised levels of serum procalcitonin (PCT), with a total material cost of £1.14. The SPA is designed to include six graphitic working electrodes with a common counter and reference electrode. The screen-printing methodology produced SPAs with an inter-array reproducibility of 3.64% and 5.51% for the electrochemically active surface area and heterogenous electrochemical rate constant respectively. The SPAs were modified with antibodies specific for the detection of PCT through a facile droplet modification methodology, where a carboxyl-terminated aryl group is covalently attached to the graphitic working electrode through the application of two droplets of solution. Using EDC/NHS coupling chemistry, the antibody is then attached to the carboxyl group through two separate droplets, removing the chance of inter-antibody coupling. This platform was used for the detection of PCT, achieving a linear dynamic range between 1 and 10 ng mL^{-1} with a sensor sensitivity of 1.35×10^{-10} NIC%/ng mL^{-1}. The SPA produced and intra- and inter-day %RSD of 4.00 and 5.05%. For serum sample measurements, three working electrodes are used to analyse the sample (n = 3) and three are used as a control (n = 3). This system gave internally validated serum results for raised levels of PCT (>2 ng mL^{-1}), with no interference seen from other proteins CRP and IL-6. This SPA platform has the potential to offer clinicians vital information to rapidly begin treatment for possibly septic patients while blood samples are transferred for analysis. Additionally, due to the facile modification methods, we predict this could be used for various analytes on a single array, or the array increased further to maintain the internal validation of the system.

CRediT authorship contribution statement

Paulo Roberto de Oliveira: Methodology, Validation, Formal analysis, Investigation, Writing – original draft, Writing – review & editing. **Robert D. Crapnell:** Conceptualization, Methodology, Validation, Formal analysis, Investigation, Writing – original draft, Writing – review & editing, Supervision. **Alejandro Garcia-Miranda Ferrari:** Formal analysis, Investigation, Writing – original draft. **Phatsawit Wuamprakhon:** Formal analysis, Investigation. **Nicholas J. Hurst:** Formal analysis, Investigation. **Nina C. Dempsey-Hibbert:** Writing – review & editing. **Montree Sawangphruk:** Investigation. **Bruno Campos Janegitz:** Writing – original draft, Writing – review & editing. **Craig E. Banks:** Conceptualization, Methodology, Validation, Formal analysis, Investigation, Writing – original draft, Writing – review & editing, Supervision, Project administration, Funding acquisition.

Declaration of competing interest

The authors declare that they have no known competing financial interests or personal relationships that could have appeared to influence the work reported in this paper.

Data availability

Data will be made available on request.

Acknowledgments

The authors are grateful to the Brazilian agencies FAPESP (2017/21097-3, 2019/00473-2, 2021/07989-4 and 22/01601-7), CAPES (001), CAPES (88887.636021/2021–00, and 001, 88887.712315/2022–00), and CNPq (303338/2019-9) for the financial support. PW thanks the Vidyasirimedhi Institute of Science and Technology (VISTEC) for financial support.

Appendix A. Supplementary data

Supplementary data to this article can be found online at https://doi.org/10.1016/j.bios.2023.115220.

References

Ariño, C., Banks, C.E., Bobrowski, A., Crapnell, R.D., Economou, A., Królicka, A., Pérez-Ràfols, C., Soulis, D., Wang, J., 2022. Electrochemical stripping analysis. Nat. Rev. Method. Primers 2 (1), 1–18.

Bard, A.J., Faulkner, L.R., White, H.S., 2022. Electrochemical Methods: Fundamentals and Applications. John Wiley & Sons.

Blume, R., Rosenthal, D., Tessonnier, J.P., Li, H., Knop-Gericke, A., Schlögl, R., 2015. Characterizing graphitic carbon with X-ray photoelectron spectroscopy: a step-by-step approach. ChemCatChem 7 (18), 2871–2881.

Chen, R., Du, X., Cui, Y., Zhang, X., Ge, Q., Dong, J., Zhao, X., 2020. Vertical flow assay for inflammatory biomarkers based on nanofluidic channel array and SERS nanotags. Small 16 (32), 2002801.

Chiesa, C., Panero, A., Rossi, N., Stegagno, M., Giusti, M.D., Osborn, J.F., Pacifico, L., 1998. Reliability of procalcitonin concentrations for the diagnosis of sepsis in critically ill neonates. Clin. Infect. Dis. 26 (3), 664–672.

Compton, R.G., Banks, C.E., 2018. Understanding Voltammetry. World Scientific.

Crapnell, R.D., Banks, C.E., 2021a. Electroanalytical overview: the pungency of Chile and chilli products determined via the sensing of capsaicinoids. Analyst 146 (9), 2769–2783.

Crapnell, R.D., Banks, C.E., 2021b. Electroanalytical overview: utilising micro-and nano-dimensional sized materials in electrochemical-based biosensing platforms. Microchim. Acta 188 (8), 1–23.

Crapnell, R.D., Banks, C.E., 2021c. Perspective: what constitutes a quality paper in electroanalysis? Talanta Open 4.

Crapnell, R.D., Banks, C.E., 2022. Electroanalytical overview: the determination of manganese. Sens. Act. Rep., 100110

Crapnell, R.D., Tridente, A., Banks, C.E., Dempsey-Hibbert, N.C., 2021a. Evaluating the possibility of translating technological advances in non-invasive continuous lactate monitoring into critical care. Sensors 21 (3), 879.

Crapnell, R.D., Banks, C.E., 2021b. Electroanalytical overview: the electroanalytical detection of theophylline. Talanta Open 3, 100037.

Crapnell, R.D., Jesadabundit, W., García-Miranda Ferrari, A., Dempsey-Hibbert, N.C., Peeters, M., Tridente, A., Chailapakul, O., Banks, C.E., 2021c. Toward the rapid diagnosis of sepsis: detecting Interleukin-6 in blood plasma using functionalized screen-printed electrodes with a thermal detection methodology. Anal. Chem. 93 (14), 5931–5938.

Crapnell, R., Ferrari, A.G.-M., Dempsey, N., Banks, C.E., 2022. Electroanalytical Overview: screen-printed electrochemical sensing platforms for the detection of vital cardiac, cancer and inflammatory biomarkers. Sens. Diagn. 1, 405–428.

Crapnell, R.D., Dempsey, N.C., Sigley, E., Tridente, A., Banks, C.E., 2022. Electroanalytical point-of-care detection of gold standard and emerging cardiac biomarkers for stratification and monitoring in intensive care medicine-a review. Microchim. Acta 189 (4), 1–48.

Dandona, P., Nix, D., Wilson, M.F., Aljada, A., Love, J., Assicot, M., Bohuon, C., 1994. Procalcitonin increase after endotoxin injection in normal subjects. J. Clin. Endocrinol. Metabol. 79 (6), 1605–1608.

de Jong, E., van Oers, J.A., Beishuizen, A., Vos, P., Vermeijden, W.J., Haas, L.E., Loef, B. G., Dormans, T., van Melsen, G.C., Kluiters, Y.C., 2016. Efficacy and safety of procalcitonin guidance in reducing the duration of antibiotic treatment in critically ill patients: a randomised, controlled, open-label trial. Lancet Infect. Dis. 16 (7), 819–827.

Faix, J.D., 2013. Biomarkers of sepsis. Crit. Rev. Clin. Lab Sci. 50 (1), 23–36.

Fang, J., Li, J., Feng, R., Yang, L., Zhao, L., Zhang, N., Zhao, G., Yue, Q., Wei, Q., Cao, W., 2021. Dual-quenching electrochemiluminescence system based on novel acceptor CoOOH@ Au NPs for early detection of procalcitonin. Sensor. Actuator. B Chem. 332, 129544.

Ferrari, A.G.-M., Carrington, P., Rowley-Neale, S.J., Banks, C.E., 2020. Recent advances in portable heavy metal electrochemical sensing platforms. Environ. Sci.: Water Res. Technol. 6 (10), 2676–2690.

Ferrari, A.G.-M., Crapnell, R.D., Banks, C.E., 2021a. Electroanalytical overview: electrochemical sensing platforms for food and drink safety. Biosensors 11 (8), 291.

Ferrari, A.G.-M., Rowley-Neale, S.J., Banks, C.E., 2021b. Screen-printed electrodes: transitioning the laboratory in-to-the field. Talanta Open 3, 100032.

Ferrari, A.G.-M., Crapnell, R.D., Adarakatti, P.S., Suma, B., Banks, C.E., 2022. Electroanalytical overview: the detection of chromium. Sens. Act. Rep. 4, 100116.

Fleischmann, C., Scherag, A., Adhikari, N.K., Hartog, C.S., Tsaganos, T., Schlattmann, P., Angus, D.C., Reinhart, K., 2016. Assessment of global incidence and mortality of hospital-treated sepsis. Current estimates and limitations. Am. J. Respir. Crit. Care Med. 193 (3), 259–272.

Foster, C.W., Metters, J.P., Kampouris, D.K., Banks, C.E., 2014. Ultraflexible screen-printed graphitic electroanalytical sensing platforms. Electroanalysis 26 (2), 262–274.

Fukuzumi, N., Osawa, K., Sato, I., Iwatani, S., Ishino, R., Hayashi, N., Iijima, K., Saegusa, J., Morioka, I., 2016. Age-specific percentile-based reference curve of serum procalcitonin concentrations in Japanese preterm infants. Sci. Rep. 6 (1), 23871.

Galdino, F.E., Smith, J.P., Kwamou, S.I., Kampouris, D.K., Iniesta, J., Smith, G.C., Bonacin, J.A., Banks, C.E., 2015. Graphite screen-printed electrodes applied for the accurate and reagentless sensing of pH. Anal. Chem. 87 (23), 11666–11672.

García-Miranda Ferrari, A., Foster, C.W., Kelly, P.J., Brownson, D.A., Banks, C.E., 2018. Determination of the electrochemical area of screen-printed electrochemical sensing platforms. Biosensors 8 (2), 53.

Gengenbach, T.R., Major, G.H., Linford, M.R., Easton, C.D., 2021. Practical guides for x-ray photoelectron spectroscopy (XPS): interpreting the carbon 1s spectrum. J. Vac. Sci. Technol.: Vacuum, Surfaces, and Films 39 (1), 013204.

González, M.C.R., Brown, A., Eyley, S., Thielemans, W., Mali, K.S., De Feyter, S., 2020. Self-limiting covalent modification of carbon surfaces: diazonium chemistry with a twist. Nanoscale 12 (36), 18782–18789.

Greczynski, G., Hultman, L., 2021. The same chemical state of carbon gives rise to two peaks in X-ray photoelectron spectroscopy. Sci. Rep. 11 (1), 1–5.

Hallam, P.M., Kampouris, D.K., Kadara, R.O., Banks, C.E., 2010. Graphite screen printed electrodes for the electrochemical sensing of chromium (VI). Analyst 135 (8), 1947–1952.

Hernández-Rodríguez, J.F., Rojas, D., Escarpa, A., 2020. Electrochemical sensing directions for next-generation healthcare: trends, challenges, and frontiers. Anal. Chem. 93 (1), 167–183.

Honeychurch, K.C., Piano, M., 2018. Electrochemical (bio) sensors for environmental and food analyses. MDPI 8, 57.

Jones, N., Tridente, A., Dempsey-Hibbert, N.C., 2021. Immature platelet indices alongside procalcitonin for sensitive and specific identification of bacteremia in the intensive care unit. Platelets 32 (7), 941–949.

Kokorina, A.A., Ponomaryova, T.S., Goryacheva, I.Y., 2021. Photoluminescence-based immunochemical methods for determination of C-reactive protein and procalcitonin. Talanta 224, 121837.

Kumar, A., Roberts, D., Wood, K.E., Light, B., Parrillo, J.E., Sharma, S., Suppes, R., Feinstein, D., Zanotti, S., Taiberg, L., 2006. Duration of hypotension before initiation of effective antimicrobial therapy is the critical determinant of survival in human septic shock. Crit. Care Med. 34 (6), 1589–1596.

La, M., 2020. Electrochemical, electrochemiluminescent and photoelectrochemical immunosensors for procalcitonin detection: a review. Int. J. Electrochem. Sci. 15, 6436–6447.

Lautz, A.J., Dziorny, A.C., Denson, A.R., O'Connor, K.A., Chilutti, M.R., Ross, R.K., Gerber, J.S., Weiss, S.L., 2016. Value of procalcitonin measurement for early evidence of severe bacterial infections in the pediatric intensive care unit. J. Pediatr. 179, 74–81. e72.

Liu, D., Su, L., Han, G., Yan, P., Xie, L., 2015. Prognostic value of procalcitonin in adult patients with sepsis: a systematic review and meta-analysis. PLoS One 10 (6), e0129450.

Malik, M., Nair, A.S., Illango, J., Siddiqui, N., Gor, R., Fernando, R.W., Hamid, P., 2021. The advancement in detecting sepsis and its outcome: usefulness of procalcitonin in diagnosing sepsis and predicting fatal outcomes in patients admitted to intensive care unit. Cureus 13 (4).

Mannino, S., Wang, J., 1992. Electrochemical methods for food and drink analysis. Electroanalysis 4 (9), 835–840.

Meisner, M., Tschaikowsky, K., Hutzler, A., Schick, C., Schmidt, J., 1998. Postoperative plasma concentrations of procalcitonin after different types of surgery. Crit. Care 2, 1–60. Springer.

Moyer, M.W., 2012. New biomarkers sought for improving sepsis management and care. Nat. Med. 18 (7), 999.

Naramura, T., Tanaka, K., Inoue, T., Imamura, H., Yoshimatsu, H., Mitsubuchi, H., Nakamura, K., Iwai, M., 2020. New reference ranges of procalcitonin excluding respiratory failure in neonates. Pediatr. Int. 62 (10), 1151–1157.

Nellaiappan, S., Mandali, P.K., Prabakaran, A., Krishnan, U.M., 2021. Electrochemical immunosensors for quantification of procalcitonin: progress and prospects. Chemosensors 9 (7), 182.

Partington, L.I., Atkin, S.L., Kilpatrick, E.S., Morris, S.H., Piper, M., Lawrence, N.S., Wadhawan, J.D., 2018. Electrochemical measurement of antibody-antigen recognition biophysics: thermodynamics and kinetics of human chorionic gonadotropin (hCG) binding to redox-tagged antibodies. J. Electroanal. Chem. 819, 533–541.

Patnaik, R., Azim, A., Mishra, P., 2020. Should serial monitoring of procalcitonin be done routinely in critically ill patients of ICU: a systematic review and meta-analysis. J. Anaesthesiol. Clin. Pharmacol. 36 (4), 458.

Pérez-Fernández, B., Costa-García, A., Muñiz, A.d. l.E.-., 2020. Electrochemical (bio) sensors for pesticides detection using screen-printed electrodes. Biosensors 10 (4), 32.

Pierrakos, C., Vincent, J.-L., 2010. Sepsis biomarkers: a review. Crit. Care 14 (1), 1–18.

Qi, X., Huang, Y., Lin, Z., Xu, L., Yu, H., 2016. Dual-quantum-dots-labeled lateral flow strip rapidly quantifies procalcitonin and C-reactive protein. Nanoscale Res. Lett. 11 (1), 1–8.

Sachse, C., Dressler, F., Henkel, E., 1998. Increased serum procalcitonin in newborn infants without infection. Clin. Chem. 44 (6), 1343–1344.
Sener, G., Ozgur, E., Rad, A.Y., Uzun, L., Say, R., Denizli, A., 2013. Rapid real-time detection of procalcitonin using a microcontact imprinted surface plasmon resonance biosensor. Analyst 138 (21), 6422–6428.
Singer, M., Deutschman, C.S., Seymour, C.W., Shankar-Hari, M., Annane, D., Bauer, M., Bellomo, R., Bernard, G.R., Chiche, J.-D., Coopersmith, C.M., 2016. The third international consensus definitions for sepsis and septic shock (Sepsis-3). JAMA 315 (8), 801–810.
Smith, S.E., Muir, J., Kalabalik-Hoganson, J., 2020. Procalcitonin in special patient populations: guidance for antimicrobial therapy. Am. J. Health Syst. Pharm. 77 (10), 745–758.
Soni, N.J., Samson, D.J., Galaydick, J.L., Vats, V., Huang, E.S., Aronson, N., Pitrak, D.L., 2013. Procalcitonin-guided antibiotic therapy: a systematic review and meta-analysis. J. Hosp. Med. 8 (9), 530–540.
Vinoth, S., Devi, K.S., Pandikumar, A., 2021. A comprehensive review on graphitic carbon nitride based electrochemical and biosensors for environmental and healthcare applications. TrAC, Trends Anal. Chem. 140, 116274.
Wacker, C., Prkno, A., Brunkhorst, F.M., Schlattmann, P., 2013. Procalcitonin as a diagnostic marker for sepsis: a systematic review and meta-analysis. Lancet Infect. Dis. 13 (5), 426–435.
Whittingham, M.J., Hurst, N.J., Crapnell, R.D., Garcia-Miranda Ferrari, A., Blanco, E., Davies, T.J., Banks, C.E., 2021. Electrochemical improvements can Be realized via shortening the length of screen-printed electrochemical platforms. Anal. Chem. 93 (49), 16481–16488.
Zhu, K., Chen, J., Hu, J., Xiong, S., Zeng, L., Huang, X., Xiong, Y., 2022. Low-sample-consumption and ultrasensitive detection of procalcitonin by boronate affinity recognition-enhanced dynamic light scattering biosensor. Biosens. Bioelectron. 200, 113914.